ELSEVIER

Polymer 43 (2002) 7419–7427

polymer

www.elsevier.com/locate/polymer

Micromechanics of stress relaxation in amorphous glassy PMMA part II: application of the RT model

L.A. Pfister[a], Z.H. Stachurski[b,*]

[a]*Department of Materials, ETH-Z, Zürich CH-8092, Switzerland*
[b]*Department of Engineering, FEIT, Australian National University, Canberra, ACT 0200, Australia*

Received 6 February 2002; received in revised form 23 September 2002; accepted 26 September 2002

Abstract

This paper describes computer simulations and experimental results of stress relaxation carried out in polymethyl methacrylate (PMMA). The results are analysed in terms of the RT model proposed earlier. The main theoretical result is that transitions of side-groups, or parts thereof, can account for approximately 10% of stress relaxation. The experimentally observed relaxation strength in a time of approximately 3 h at 50 K below T_g is of the order of 40–60%. These facts provide conclusive evidence that cooperative motions of main chain segments are responsible for most of the stress relaxation. A qualitative model for stress relaxation due to chain twisting is described and shown capable of large stress losses. © 2002 Published by Elsevier Science Ltd.

Keywords: PMMA nano-structure; Stress relaxation; RT model

1. Introduction

The recent book on 'Group Interaction Modelling of Polymer Properties' [1] is an indication of the importance of this field of research in both academic and practical sense. However, the understanding of mechanical relaxations in amorphous polymers is still incomplete due to the inadequacy of quantitative models based on structural information. A number of publications [2–6] point to the need for a better relationship between the polymer structure and the corresponding relaxation's strength and time spectrum. A novel approach, based on measured and characterised polymer nano-structure, arose with the improvements of computer simulations of amorphous polymers [7,8]. In a previous publication, a so-called RT model was proposed for mechanical relaxation in an un-oriented, isotropic amorphous polymer, which contains chains with rotating side-groups [9]. A relationship for the stress relaxation modulus was derived, expressed in the following general form:

$$E_{\text{relax}}(t,T,\Omega) = E_{\text{U}}(T,\Omega) - \Delta E(\Omega) \times H(t,T,\Omega) \tag{1}$$

where E_{U} is the unrelaxed value of the modulus, and the variables in the round brackets indicate functional dependence on time t, temperature T, and structure Ω. The maximum relative relaxation strength for a specific motion, $\Delta E/E_{\text{U}}$ (for $t \to \infty$), was derived from the geometry of packing of individual side-groups capable of stress relaxation, and its value was predicted in terms of molecular parameters as follows:

$$\frac{\Delta E}{E_{\text{U}}} = \frac{1}{\pi} \times \frac{\bar{d}}{\bar{\Phi}} \times \frac{\bar{V}_{\text{NAS}}}{\bar{V}_{\text{mon}}} \tag{2}$$

Both, the second and third terms include quantities measured from the nano-structure of the polymer (albeit only simulated at this stage). The detailed relationships for the dependence of the relaxation spectrum on time, and on specific nano-structural features characteristic of the state of the polymer, were expressed as follows:

$$H(t,T,\Omega) = \sum_{i=1}^{N} p_i(\tau_{\text{R}}) \left[1 - \exp\left(-\frac{t}{(\tau_{\text{R}})_i} \right) \right] \tag{3}$$

$$\tau_{\text{R}}(T,x) = \tau_0 \exp\left(\frac{Q_1}{k_{\text{B}}T} \right) \exp\left(\frac{q_2/x}{k_{\text{B}}T} \right) \tag{4}$$

where p_i is the fractional relaxation strength associated with an ith relaxation time, subject to the normalization: $\sum p_i = 1$ for $i = 1$ to N. The structural parameter, $x = (V_{\text{mon}} - V_0)/V_0$, is a subset of Ω. The latter quantity is not defined

* Corresponding author. Tel.: +61-2-6125-5681; fax: +61-2-6125-0506.
E-mail address: zbigniew.stachurski@anu.edu.au (Z.H. Stachurski).

0032-3861/02/$ - see front matter © 2002 Published by Elsevier Science Ltd.
PII: S0032-3861(02)00689-4

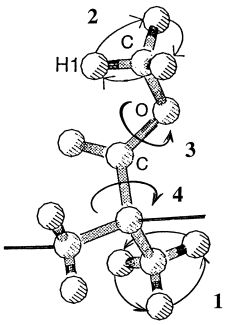

Fig. 1. The four side-group rotational motions on PMMA monomer that can contribute to mechanical stress relaxation through the RT mechanism [9].

specifically at this stage. N is the number of discrete relaxation times, and each discrete relaxation time is a function of temperature. The constant, τ_0, is the quantum time constant of oscillations of the atomic group around a fixed bond, Q_1 is the activation energy for rotational relaxation unrestricted by neighbouring chain segments (i.e. isolated chain in solution), and finally, q_2 is the additional activation energy due to the presence of neighbouring chain segments (i.e. due to polymer structure). The sum, $Q_1 + q_2/x$, is the energy activation barrier, E_{barrier}.

The relaxation modulus shows manifold dependencies: (i) a one-dimensional dependence on time, (ii) a two-dimensional dependence on temperature (through relaxation times and density), and (iii) a three-dimensional dependence on structure (through relaxation strength in Eq. (2), dependence on fractional strength p_i, and on the parameter, x, in Eq. (4). The model lends itself to quantitative calculations and predictions based on results from simulated polymer cells, and the results included here allow some verification of the model and several significant conclusions to be made.

2. Computer simulation of amorphous PMMA cell

2.1. Amorphous cell and Voronoi tessellation

Following the method of Suter et al. [10], amorphous polymer cells were simulated using Materials Studio software (Molecular Simulations Inc., San Diego, USA). An amorphous PMMA cell at a density of 1.12 g/cm^3, with a cube edge length of 3.55 nm, was formed at 328 K (approx. 50 °C below T_g) comprising three chains with 100 monomers each (MW = 10 012), a total of 4602 atoms. First, the three chains were generated in a stretched conformation by the use of the default polymer builder. Next, the amorphous cell was constructed from an initial density of 0.6 g/cm^3 and minimized in size towards the target density. Short molecular dynamics (MD) runs were carried out within the same process. This roughly equilibrated structure was further minimized in 5000 steps before the full MD run with approximately 80,000 steps (0.08 ns).

Analysis of the conformations of all monomers showed that the ester groups were in the 'folded' position, that is, the C–O bond is in the trans position and the terminal methyl group is situated between the two oxygen atoms. This is in accordance with published NMR measurements [11]. The average potential energy of the simulated PMMA was 61.8 kJ/mol and stayed within (0.5% during the last 30 ps of the simulation, indicating a structure in adequate equilibrium. The potential energy is slightly higher than that quoted in literature (57 kJ/mol), which could be due to the configuration of the simulated cell.

PMMA has four identifiable side-group motions, as shown in Fig. 1; each can contribute an RT-type relaxation. Voronoi tessellation for all atoms was carried out using a specially written software routine [12]. The Voronoi volumes of each monomer, and each side-group, or part thereof, were calculated by adding up the volumes of their respective atoms. Some of the results are shown in Figs. 2–4. Fig. 2 shows the Voronoi volumes for each of the monomers for the three chains. The horizontal lines indicate (from top) average monomer volume: (i) at T_g, (ii) at 328 K, and (iii) extrapolated to absolute zero (0 K). There appears to be an underlying periodicity in the variation of volume, with an amplitude of the order of 20×10^{-3} nm^3, with superimposed random spikes, both positive and negative, reaching approximately from 121×10^{-3} nm^3 up to as high as 197×10^{-3} nm^3. The frequency distribution is shown in Fig. 3. Such an inhomogeneity at the nano-scale of atomic dimensions can be expected to result from considerations of the geometry and topology of randomly packed chains of limited flexibility [13]. The Voronoi volumes for each of the methyl groups of both type, and each of the $COOCH_3$ side-groups for the three chains, are shown in Fig. 4(a)–(c). The Voronoi volumes of hydrogen and oxygen atoms, although not included here, also show similar variations with underlying apparent periodicity as well as randomness. Similarity can be observed between the graphs in Figs. 2 and 4, even though the side groups, being on the outside of the chain, can participate more directly in sharing the inter-chain space where free volume is to be found. The average Voronoi volumes, and the Van der Waals volumes of selected molecular assemblies, are summarized in Table 1.

2.2. Molecular parameters

The average monomer Voronoi volume for PMMA at 328 K is 148.2×10^{-3} nm^3. The monomer length was measured and found to be 0.274($\pm$0.001) nm; the average chain diameter was calculated to be, $\Phi = 0.769$ nm. The net atomic sets (NAS) for each rotating side-group were identified. It was assumed that when a group flips from one site to another, it always rotates by 180°, which yields the maximum local stress relaxation. For group No. 1, 2H rotate around C–C bond and exchange place with H,

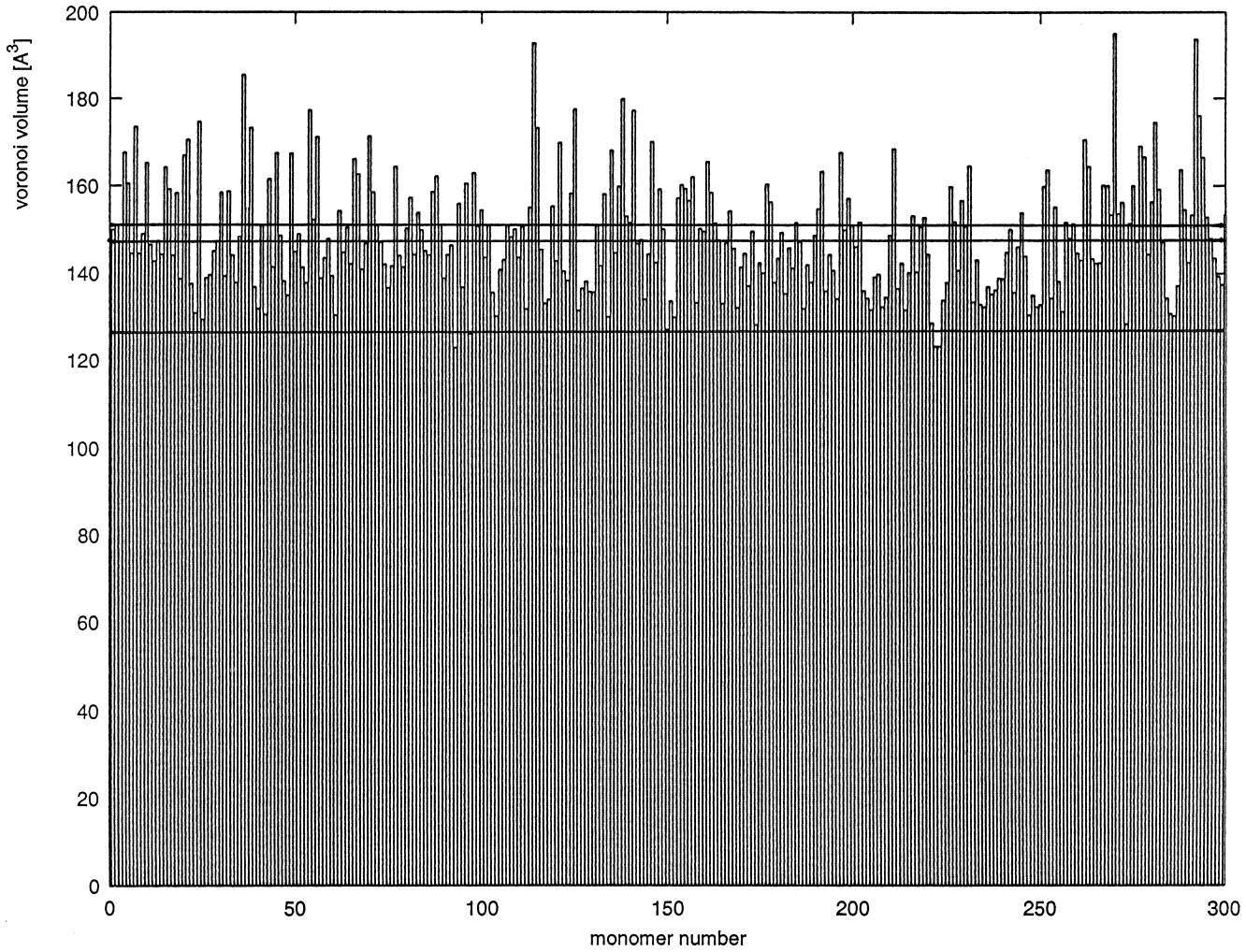

Fig. 2. Sequential monomer Voronoi volumes for the three PMMA chains. The horizontal lines indicate average volumes (from top): at 378 K (T_g), at 328 K (simulation temperature), and at 0 K (extrapolated).

therefore NAS = H. For group No. 2, 2H rotate around O–C bond and exchange place with H, therefore NAS = H. For group No. 3, CH_3 rotates around C–O bond and exchanges place with void space, therefore NAS = CH_3. For group No. 4, O–CH_3 rotates around the C–C bond and exchanges place with O=, therefore (to a good approximation) NAS = CH_3. The list of the side-groups and their associated NAS parameters is given in Table 2.

Table 1
Voronoi and van der Waals volumes of selected atomic groups in PMMA

Group	Voronoi (Å^3)		van der Waals (Å^3)
	V_{328}	V_0	V_{VdW}
Monomer	148.4	135.2	93.1
$-COOCH_3$	78.3	71.3	47.9
CH_3 in $-COO-CH_3$	46.8	42.6	22.7
CH_3 on main chain	39.3	35.8	22.7

V_{328} determined by Voronoi tessellation, V_0 calculated Voronoi volume by application of volumetric thermal expansion coefficient of 2.7×10^4 K, V_{VdW}: Van der Waals volumes obtained from vanKrevelen [29].

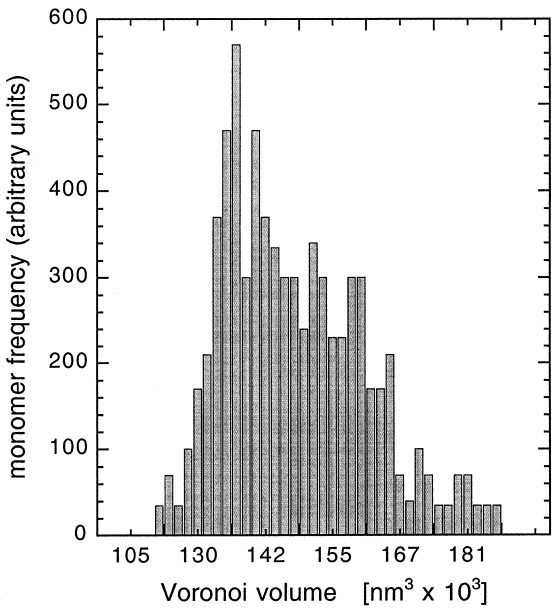

Fig. 3. Distribution of monomer Voronoi volumes obtained from the data in Fig. 2.

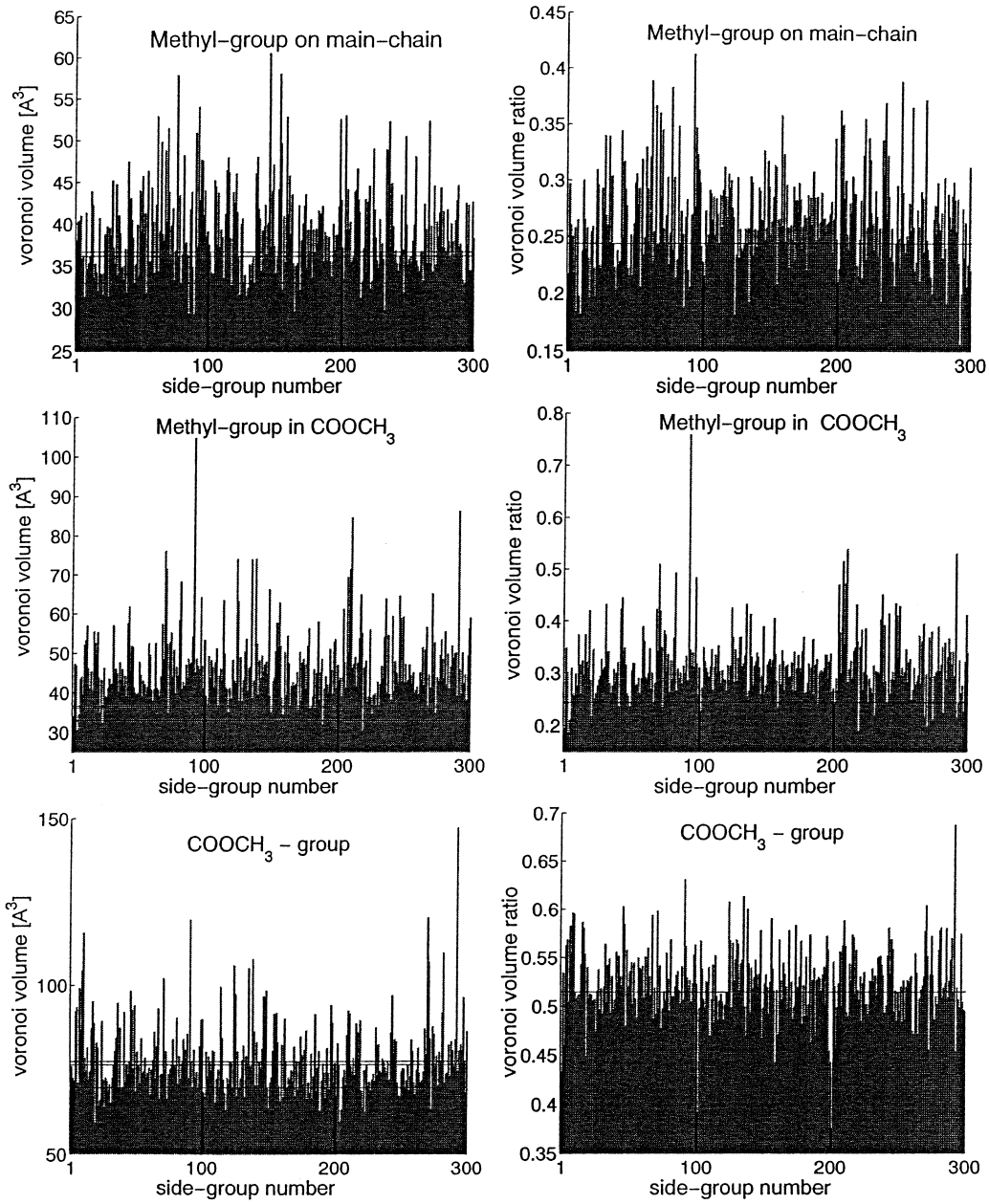

Fig. 4. On the left-hand side, Voronoi volumes for side groups on PMMA monomers. On the right-hand side, ratios of the side group Voronoi volumes to corresponding monomer Voronoi volumes.

The average displacement vector, d, is the vector from the centre of the Voronoi volume of a NA set in site 1 to its new site 2, after a rotation of 180°. The calculation of d requires the knowledge of the distance between the centre of the Voronoi volume and the atoms of the side-group, the orientation of the centre with respect to the side-group, and the change in orientation and distance after the rotation. Since these values cannot be derived form our data, we have used simplified estimations based on the following assumptions:

1. The Voronoi volume is in the shape of a sphere and is attached to the Van der Waals volume, V_{VdW}, of the NA set (also represented by a sphere) in such a way that it encloses V_{VdW} and points outwards with respect to the monomer.
2. For both methyl-groups and for the OCH_3 group, the

Table 2
Geometric and mechanical parameters for NAS in PMMA

RT motion	NAS	V_{NAS} (Å^3)	V_{NAS}/V_{mon}	d (Å)	$\Delta E/E$
1	H	12.05	0.081	2.4	0.81×10^{-2}
2	H	14.62	0.098	2.6	1.05×10^{-2}
3	CH_3	46.8	0.316	2.7	3.52×10^{-2}
4	CH_3	46.8	0.316	3.2	4.17×10^{-2}

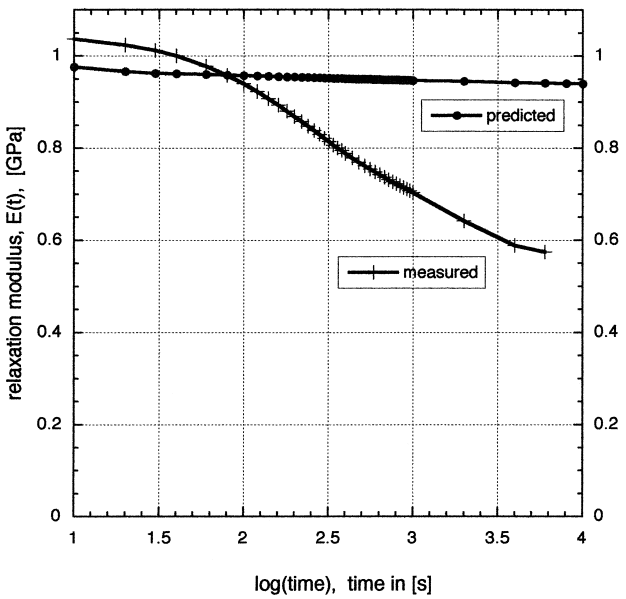

Fig. 5. Relaxation modulus of PMMA as a function of log(time). Measured curve from stress relaxation experiment (at a strain of 4%). Predicted curve from Eqs. (1)–(4) and data from Tables 2 and 3. The unrelaxed value of the relaxation modulus was assumed as 1 GPa at $t = 0$, and $T = 0$ K.

centre is assumed to be on the elongation of the bond between the side-group and the atom it is attached to. The bond length is then taken to be $(V_{mon}/V_{VdW})^{-1/3}$ times the initial bond length.

3. The CH_3 for the rotation of the $COOCH_3$ group is supposed to be in the folded position, i.e. it is in the plane spanned by the COO and situated between the two oxygen. Given a straight line perpendicular to the longitudinal monomer axis and through the NA set, the centre of the Voronoi volume is then estimated to be on a circle with radius extending from the centre of the NA set atoms and under an angle of 0° to 90° away from the double-bonded oxygen. This leads to an increment of the displacement vector (measured from the initial atom centre to the new one) of about 0 to $0.22 \times (V_{mon}/V_{VdW})^{-1/3}$ nm. Since the angle is not known precisely, an average increment of $0.1 \times (V_{mon}/V_{VdW})^{-1/3}$ was chosen.

A summary of the relevant molecular parameters is shown in Table 2.

3. Experimental measurement of stress relaxation

3.1. Materials and methods

The PMMA material was made by ICI as cast sheet ($2.8 \times 2000 \times 2500$ mm^3) and purchased from a selling agent for Australia. The specimens, in the shape of standard samples (ASTM D638), were mill-cut from the PMMA plate. The plates had been annealed at room temperature for over 10,000 h so that a good equilibrium of the material can be assumed. A specimen was typically 2.8 mm thick with a width of 20 mm at both ends and 12.8 mm in the middle. The gauge length was 50 mm. The relaxation and tensile tests were carried out on a universal testing machine (Instron 4505). One of the crucial factors of relaxation experiments is the control of temperature. A special box with heater was built to run experiments at elevated temperatures. The temperature was monitored with a thermocouple on each side of and close to the specimen. To obtain a uniform temperature, a small fan was placed in the box, pointing from the up-right corner towards the bottom. In addition, an aluminium sheet was placed in front of the heater to prevent the current of hot air blowing directly at the specimen. The heater was connected to a Variac transformer that allowed control of temperature in the box by adjusting the voltage. With this set-up it was possible to keep the temperature within 1 °C during the experiments.

3.2. Relaxation measurements

The relaxation experiments were carried out at a temperature of 328 K. The box and the specimen were preheated for 1–2 h. The box was opened, the specimen inserted into the clamps and the window closed again. The stress on the specimen that had been applied during the tightening of the clamps, was eliminated by slowly moving the crosshead until the stress dropped below 1 MPa. It was kept between ±1 MPa (corresponding to approx. ±5 N force) until the default temperature was reached again, which took about 5–8 min. Then, the test was started.

The crosshead was moved downwards with a speed of 50 mm/min until the prior set extension was reached. A 5 kN load cell was used with an accuracy of 0.5% of indicated load. The elongation was measured by the movement of the crosshead with an accuracy of 0.1%. No extensometer was used. The displacement was usually held for 3 h and the stress was recorded with a rate of 12.5 pts/s for the first minute, and then reduced by a factor of 18, exploiting the maximum amount of sampling points (8000). Fig. 5 shows a typical result of the stress relaxation modulus, which is in agreement with previously published data.

4. Application of the RT model to PMMA

4.1. Maximum relaxation strength

Substitution of the appropriate data appearing in Table 2 into Eq. (2) leads to the following calculation for the relaxation strength due to CH_3 net atomic set group (motion 4, rotation of the ester group around the C–C bond,):

$$\frac{\Delta E}{E} = \frac{1}{\pi} \times \frac{0.32}{0.769} \times \frac{46.8}{148.4} = 4.2 \times 10^{-2} \quad (5)$$

Table 3
Molecular dynamic parameters for net atomic (NA) sets in PMMA

RT motion	Q_1 (kcal/mol)	q_2 (kcal/mol)	τ_0 (s)	$\tau_R(x=\infty)$ (s)	$\tau_R(x=0.15)$ (s)
1	2.1	0.4	6.5×10^{-12}	2.2×10^{-10}	2.3×10^{-10}
2	2.1	0.4	6.5×10^{-12}	2.2×10^{-10}	2.3×10^{-10}
3	10	2.0	42.3×10^{-12}	7.3×10^{-4}	1.2×10^{-3}
4	12	2.0	109×10^{-12}	5.3×10^{-2}	8.7×10^{-2}

This represents the maximum possible relaxation strength due to rotation of the whole ester group. Similar calculations, carried out for the remaining three possible RT motions, yielded the values shown in the last column of Table 2. Assuming that the relaxation strengths for each RT motion are additive, the sum of the four is close to 0.096. This means that relaxation by all side-groups in an amorphous, isotropic PMMA can account for nearly 10% drop of the unrelaxed modulus (at sufficiently long time). The value of the unrelaxed modulus can be obtained by theoretical calculations [14], or from experimental measurements [15]. Since the aim here is to demonstrate the predictive ability of the model, rather than any specific values, then the actual precise value is not important, and a nominal value of 1 GPa was chosen.

4.2. Relaxation spectrum and modulus

The predicted modulus decay shows a very broad relaxation over the time interval from 1 to 10^4 s (~3 h). At the shortest measured time the relaxation modulus has already dropped to approximately 0.98 GPa due to relaxations of the methyl groups (motions 1 and 2), which have a very short relaxation time (Table 3). At the longest time of 10^4 s, the modulus has lowered to a value of 0.92 GPa, indicating that most of the stress decay by motions 3 and 4 have taken place, but not completely. The long-term tail of the relaxation spectrum, particularly for motion 4, stretches far into the 10^{10} s region, therefore providing some resistance to complete relaxation at 10^4 s.

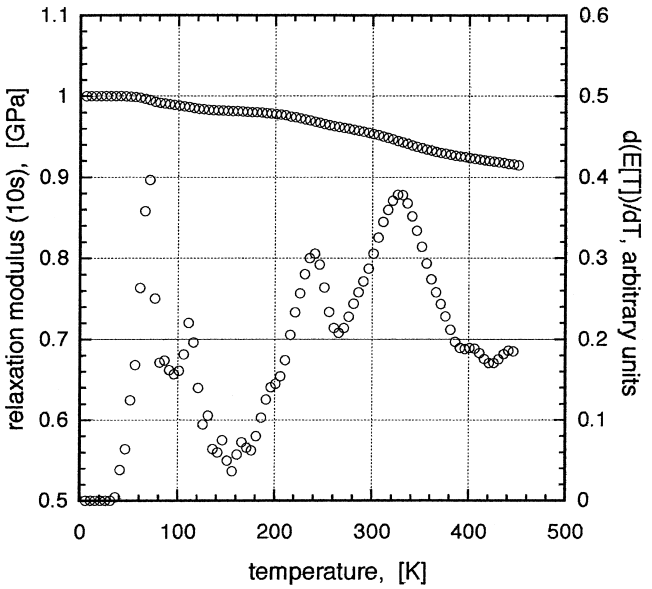

Fig. 6. Predicted relaxation modulus of PMMA as a function of temperature (top curve), and the derivative (bottom curve). Relaxation of modulus due to side-groups motions only, in accordance with the RT model [9].

Thirty eight discrete fractional relaxation strengths were derived from the distribution of Voronoi volumes shown in Fig. 3 by segregating the volumes into bins of 5×10^{-3} nm^3 size. These were used in Eq. (4) to calculate relaxation times and the corresponding relaxation time spectrum. To calculate relaxation times it was necessary to obtain values for τ_0, Q_1, and q_2. In principle, all of these quantities can be derived by quantum mechanical approach [16]. We have assumed τ_0 to be a temperature independent constant. The actual value for the methyl groups was taken from Nicholson and Davies [6] to be 6.5×10^{-12} s. The other values, shown in Table 3, were adjusted in proportion to the rotational moments of inertia of the atomic groups, and must be taken as approximate. Since thermal motions are neglected, the method will almost certainly overestimate the effects of neighbouring segments [6]. Eq. (1) has been evaluated using either time or temperature as variable. Fig. 5 shows the simulated stress relaxation modulus as a function of time at a constant temperature (328 K), and Fig. 6 shows the variation of the simulated stress relaxation modulus as a function of temperature at a constant time of 10 s. The methyl groups give a slight drop around 100 K, whereas motions of the ester groups show a significant relaxation from 200 K. These appear to correspond approximately with the α and β relaxations as indicated by the peaks of the negative derivative.

4.3. Voronoi tessellation

Looking at Fig. 2 one can observe that at some points along the molecular chain the monomers are constricted to volumes well below those corresponding to a crystalline state, even if extrapolated to 0 K. Others are surrounded by significant excess volume, well above the average value at T_g. The distribution function of the monomer Voronoi volumes, shown in Fig. 3, yields the mean of the distribution at $V=148.2\times10^{-3}$ nm^3, and its mode at $V=135\times10^{-3}$ nm^3. The lowest Voronoi monomer volume was recorded at 121×10^{-3} nm^3, and the highest at 197×10^{-3} nm^3. Such variations have been observed on simulated structures published before [17–19], and have some experimental verification from PALS [20]. Intuitively,

we are inclined to accept that this nano-structure has close resemblance to that existing in real amorphous polymers (which at present cannot be measured to the degree required for verification), and that it is characteristic of the amorphous state. Thus, Voronoi tessellation provides a method of describing the structure, analogous in some way to crystallography for ordered solids. Fig. 4 includes the calculated Voronoi volumes for the three parts of monomers, as indicated. We were surprised to discover that the ratios of the atomic subgroup's Voronoi volumes to the monomer Voronoi volumes give slightly different but qualitatively the same variations and distributions.

5. Discussion

5.1. Viscoelastic models for stress relaxation

Calculations of the type shown above, have been carried out extensively in the 1960s by Ferry and many other researchers, who studied viscoelastic behaviour of polymers. Box and wedge relaxation spectra had been applied empirically, or their shape derived from experimental data with the use of Alfrey's approximation [21]. More recently, a different approach was taken by Glen and Edward [22], who used a single relaxation time model for each of the α, β, and γ relaxations, and then applied Gaussian smear to each line, thus achieving a broad relaxation behaviour in good agreement with experiment. The Gaussian broadening can be understood as representing physically the effect of the random thermal motions.

An approach to simulations of stress relaxation from the MD point of view confirms the long held view of cooperative motions, and of changing distribution of relaxation times under deformation. MD simulations carried out on simple 2D models of polymers and metals indicate the existence of clusters [4,22], i.e. the dynamic motion of an atomic set is influenced by its immediate surrounding neighbours, providing support to the notion of the energy barrier having two components (Q_1 and q_2). Studies of the normal modes in polymer chains with freely jointed and/or retarded internal rotation show a split in relaxation times occurring as soon as the chain is deformed [5]. In a non-deformed equilibrium state, the relaxation of normal modes proceeds independent of each other. With increasing deformation, the parallel and perpendicular relaxation times both decrease and begin to differ. This result also indicates the complex nature of the dynamic environment. A study most closely related to the work presented here, is the modelling of methyl group rotations in PMMA [6]. Whereas the RT model describes the micromechanics of relaxation, the paper by Nicholson and Davies elaborates on the dynamics of the methyl group in an amorphous cell created by the same modelling tools [23]. The most important result (for us) is that transitions between the three sites were observed and that distribution of the transition rates was wide. Another important result was that activation energy barriers were affected by neighbouring chains and that as the density of the polymer was increased (hydrostatic compression) the distribution broadened. In some cases, the pressure exerted by surroundings caused a decrease of the activation barrier. Since the barrier is expressed as the difference in potential energy levels, such an effect is physically admissible and probable. This effect has also been described by Bicerano [3]. It is not entirely in line with the hypothesis put forward here that the energy barrier varies reliably with changes in structure expressed simply by the structural parameter, x, and it is evident that the structural dependence may be more complex. In the first approach to this problem, the structural parameter relates to the Voronoi volume of the monomer. However, a particular rotating group, attached to that monomer, has its own (smaller) Voronoi volume. The dynamics of this group will be more directly associated with the smaller Voronoi volume rather than the overall monomer Voronoi volume, and consequently the structural parameter should be expressed in these new terms. This has been tried using the data in Fig. 4, and found not to affect significantly the final results.

A physical method for apportioning of the energy activation barrier into the Q_1 and q_2 components should be based on: (i) the relative intra- and inter-chain surface area, and (ii) the strength of the interactions across the surface. This can be quantified by means of the group Voronoi polyhedron, of which individual faces can be identified as intra-chain or external, and by an appropriate coefficient of elastic interactions across the faces. In one respect the RT model is fundamentally different to those described in the above-mentioned publications, in that the relaxation time spectrum (including its shape) has been derived entirely from nano-structural information obtained through Voronoi tessellation and a mathematical model relating it to relaxation parameters. This is, therefore, physically a much more realistic model.

5.2. Chain twisting—motion type 5

Consider a small but representative element of the polymer sample, as shown in Fig. 7, subjected to an applied extensional strain, $\varepsilon_{\text{appl}}$. Any arbitrary length of the molecular chain is elongated or compressed along with the volumetric deformation of the sample. Such elongation will result in bending and twisting of the chain length as a consequence of it following a random, coiled configuration. A random coil subjected to affine deformation will suffer in general stretching (or compression), bending, and torsion. Maximum torsion will occur in sections which are at a greatest distance from the axis of the applied force, and whose normal vector is orthogonal to the vector parallel to the direction of maximum elongation (maximum principal stretch). Therefore, segments of every chain in amorphous polymers will suffer twisting when the polymer sample is

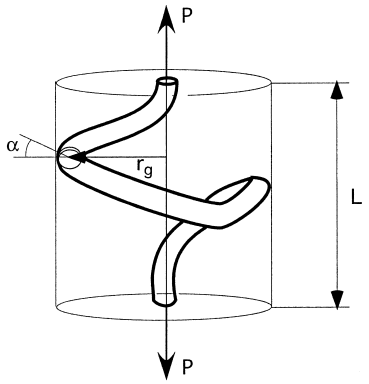

Fig. 7. A representative volume of the polymer sample showing single chain in random coil configuration. On extension, the chain can accommodate the deformation by a twist through an angle, α, at a radius r_g.

subjected to an extension. The twisting will encounter elastic resistive force resulting from the torsional stiffness of the chain and from the elastic reaction of the matrix.

After a characteristic time, τ_R, a twist relaxation will have taken place in a polymer chain. The corresponding molecular rearrangement will result in stress relaxation of a corresponding magnitude. If the twist transition occurs in a segment that is at a radius, r_g, from the axis of coil tension, then the 'internal strain', $\Delta\varepsilon'$, which contributes to the stress relaxation, is given to a good approximation by:

$$\Delta\varepsilon' \cong \alpha \times \frac{r_g}{L} \times \frac{A_{chain}}{A_{sample}} \qquad \text{for } \alpha \ll 1 \tag{6}$$

where the prime above $\Delta\varepsilon$ indicates internal strain due to one chain only, α is the angle of twist experienced by the segment at radius r_g, and A_{chain} and A_{sample} are cross-sectional areas of the chain and sample, respectively. The ratio of the areas represents the concentration, C_A, of the relaxation events. The radius, r_g, is related to L_c, the contour length of the chain, and L is shown in Fig. 7. A simple function incorporating this relationship is as follows:

$$r_g = \Phi \times \left(\frac{L_c}{L} - 1\right) \tag{7}$$

For a Gaussian coil, $L_c = nl_0$, and $L = l_0\sqrt{n}$. Substitution into Eq. (6) gives:

$$\Delta\varepsilon' \cong \alpha \times \frac{\Phi}{l_0} \times \left(1 - \frac{1}{\sqrt{n}}\right) \times \frac{A_{chain}}{A_{sample}} \tag{8}$$

The ratio, $\Phi/l_0 \cong 1$, is constant for a given polymer, and for large n the second term in the round brackets can be neglected, giving the internal strain per single chain directly related to the angle of twist. Clearly, twisting at segments less than r_g(max) is inefficient from the mechanics point of view. We note that for an imposed (applied) strain of the order of 10^{-2}, each chain need twist in only one segment by 10^{-2} radian (approx 0.6°) to comply with the deformation. Assuming that a number of chains in the sample can contribute to the extensional internal strain by similar twist transformation, then the strength of stress relaxation can be related to this mechanism as follows:

$$\frac{\Delta E(t)}{E_U} = \frac{\alpha(t) C_A}{\varepsilon_{appl}} \tag{9}$$

The development of a mathematical formulation for the maximum relaxation strength by this mechanism, and the associated relaxation spectrum, has not been completed yet. There are, however, strong reasons to believe that is it related to the existence of the density of constriction points in the microstructure of amorphous polymers, as described previously [13]. The constriction points divide each macromolecular chain into relatively short segments (for PMMA approximately nine monomers). It is the relaxations within these segments, involving motions 5, 6 and 7, that are responsible for the remaining 50% drop in the modulus, observed in Fig. 6, in addition to the 10% drop due to the RT-motions.

5.3. Structural dependence of stress relaxation

Until not so long ago, the understanding of relaxation phenomena was in terms of concepts such as the crank-shaft and Schottky rotations [24,25], or chair-transition [26,27] and others, all derived from the physical behaviour of isolated chains. The development and use of advanced computer simulation for amorphous polymer cells has changed that view. Simulations of deformation in amorphous polymers failed to confirm large-scale molecular transition [28]; instead the considerations of the complex inter-chain interactions has revealed the possibility of a multitude of local metastable positions in the potential energy phase-space. The equation below shows one comprehensive way to describe the interactions between the atoms in polymer chains [7]:

$$\begin{aligned} V(R) = {} & \sum_b D_b[1 - \exp(-a(b - b_0))]^2 + \sum_\theta H_\theta(\theta \\ & - \theta_0)^2 + \sum_\alpha H_\alpha[1 + \cos(n\alpha)] + \sum_\chi H_\chi \chi^2 \\ & + \sum_b \sum_{b'} F_{bb'}(b - b_0)(b' - b_0') + \sum_\theta \sum_{\theta'} F_{\theta\theta'}(\theta \\ & - \theta_0)(\theta' - \theta_0') + \sum_b \sum_\theta F_{b\theta}(b - b_0)(\theta - \theta_0) \\ & + \sum_\theta \sum_{\theta'} F_{\theta\theta'\alpha}(\theta - \theta_0)(\theta' - \theta_0')\cos\alpha + \sum_\chi \sum_{\chi'} \\ & \times F_{\chi\chi'}\chi\chi' + \sum_i \sum_{j>1} \left[\frac{A_{ij}}{r_{ij}^{12}} - \frac{B_{ij}}{r_{ij}^{6}} + \frac{q_i q_j}{r_{ij}} \right] \end{aligned} \tag{10}$$

The first four terms reflect the potential energy required to stretch bonds, bend angles, rotate torsion angles, and distort planar atoms out of plane. The next five terms are cross terms that account for interactions between the four types of

internal coordinates. The last term represents the non-bonded interactions between neighbouring chain segments. Although it is the third term which is primarily involved in twisting of the chain, all of the other interactions will be involved to a greater or lesser degree. In other words, the twist need not be a major conformational transition, quite unlikely to happen at infinitesimal strains. More likely is an event where slight twisting of the chain may trigger rotations of the side-groups by the RT mechanism, leading to a change in the angle, α, small enough not to cause isomeric transition, but sufficient to relax the stress and dissipate elastic stored energy. A related and accompanying mechanism for relaxation is the motion of type 6 and 7 in which a segment of the chain slips through a constriction around it. When relaxation by twisting of the chain occurs, the segment subjected to direct tension (Fig. 1) will need to slip past its neighbours to yield the internal strain, $\Delta\varepsilon'$. This provides for a gradual, and seemingly continuous mechanism, for decay of the applied stress. From the above discussion, one can infer that stress relaxation should occur for as long as chain coils are able to undergo twist motions. One may therefore ask the questions (i) why do amorphous polymers show relaxation strength of the order of 40–60% in a reasonable time interval, and not 100%, (ii) what is the molecular mechanism which prevents complete stress relaxation to zero, and consequently, (iii) why does the organic glass behave as a viscoelastic solid rather than a viscoelastic liquid. We propose that the answer to these questions can be found in the structural and topological features of amorphous polymers. Fig. 2 shows that there is a significant number of PMMA monomers with Voronoi volumes, V_{mon}, below the average value, and some are significantly below the crystalline value. In a previous publication one of the authors referred to these features as points of constriction [13]. These constitute a memory network in the relatively compliant matrix. Such constrictions provide limitations on the propagation of the motions 5, 6 and 7, thus imposing a limit on the amount of internal strain that the structure is capable of at temperatures not too far below the glass transition temperature.

6. Conclusions

Motions of side-groups, whilst clearly associated with specific mechanical relaxations (α, β), cannot be entirely and solely responsible for each relaxation. Yet, the motion of side groups is intimately associated with these relaxations. The much quoted molecular mechanisms, such as the crank-shaft motion [24,25], or the phenyl ring chair to twist-boat transition [26], or any other small atomic set motion, cannot account for the observed losses in the value of the relaxation modulus.

Voronoi tessellation provides an effective and widely accepted method for characterising amorphous polymers at the nano-structural level, and provides means for evaluating a quantitative relationship between the phenomenon of mechanical relaxation and the structural state of the polymer.

Acknowledgements

The corresponding author (ZHS) wishes to thank MSI Inc. for providing Materials Studio software free of charge for the duration of this project. One of us (LAP) has taken part in the ETH-ANU student exchange program.

References

[1] Porter D. Group interaction modelling of polymer properties. New York: Marcel Dekker; 1995.
[2] Edward GH, Glen RM. Deformation mechanism maps for poly (methyl methacrylate) and polycarbonate. Mater Forum 1987.
[3] Bicerano J. J Polym Sci-Phys 1991;29:1345.
[4] Blonski S, Brostow W, Kublat J. Phys Rev B, Condens Matter 1994; 49:924.
[5] Neelov IM, Lyulin AV, Torchinskii FI, Darinskii AA, Cooke R. Theory and mathematical modelling. Polym Sci A 1996;38(8):924. Translated from Vysokomolekularnye Soedinienya.
[6] Nicholson TM, Davies GR. Macromolecules. 1997;30:5501.
[7] Mattice WL, Suter UW. Conformational theory of large molecules—the rotational isomeric state model in macromolecular systems. New York: Wiley; 1994.
[8] Roe RJ, editor. Computer simulation of polymers. New Jersey: Prentice Hall; 1991.
[9] Stachurski ZH. Micromechanics of stress relaxation in amorphous glassy PMMA. Part I: molecular model of anelastic behaviour. Polymer 2002;43(26):7419.
[10] Theodorou D, Suter UW. Macromolecules. 1986;21:3237.
[11] Schmidt-Rohr K, Kulik AS, Beckham HW, Ohlemacher A, Pawlezik U, Boeffel C, Spiess H. Macromolecules 1994;27:4733.
[12] Lousteau B. PhD Thesis, ESPCI, Paris, France; 2000.
[13] Stachurski ZH. J Mater Sci 1986;21:3231.
[14] Gusev AA, Zhender MM, Suter UW. Phys Rev B 1996;54:1.
[15] Tobolsky AV. Properties and structure of polymers. New York: Wiley; 1960. Chapter 4.
[16] Smith VH Jr, Schaefer HF III, editors. Applied quantum chemistry. Boston: Reidel; 1986.
[17] Rigby D, Roe JR, Macromolecules . 23 1990;5312.
[18] Hutnik M, Gentile FT, Ludovice PJ, Suter UW, Argon AS. Macromolecules 1991;24:5962.
[19] Sylvester MF, Yip S, Argon AS. In: Roe RJ, editor. Computer simulation of polymers. New Jersey: Prentice Hall; 1991.
[20] Hasan OA, Boyce MC, Li XS, Berko S. J Polym Sci: B, Polym Phys 1993;31:185.
[21] Alfrey T. Mechanical properties of high polymers. New York: Interscience; 1948.
[22] Hill RM, Dissado LA. J Mater Sci 1983;19:1576.
[23] Materials Studio 2000. Molecular Simulations Inc. (presently Accelrys Inc.), San Diego, USA.
[24] Boyd RH. Polymer 1985;26:1130.
[25] McCrum NG, Read BE, Williams G. Anelastic and dielectric effects in polymeric solids. London: Wiley; 1967. p. 181.
[26] Cowie JMG. J Macromol Sci-Phys 1980;B18(4):569.
[27] Heijboer J. Mechanical properties of glassy polymers. TNO Central Laboratorium Communications No. 435, Delf, The Netherlands; 1972.
[28] Argon AS, Bulatov VV, Suter UW. J Rheol 1995;39(2):377.
[29] vanKrevelen DW. Properties of polymers. London: Elsevier; 1972.